

# Propagation of UWB pulse in two turns of meander microstrip line connected in cascade

Alexander V. Nosov

Dept. of Television and Control  
Tomsk State University of Control  
Systems and Radioelectronics  
Tomsk, Russian Federation  
alexns2094@gmail.com

Roman S. Surovtsev

Dept. of Television and Control  
Tomsk State University of Control  
Systems and Radioelectronics  
Tomsk, Russian Federation  
surovtsevrs@gmail.com

Talgat R. Gazizov

Dept. of Television and Control  
Tomsk State University of Control  
Systems and Radioelectronics  
Tomsk, Russian Federation  
talgat@tu.tusur.ru

**Abstract**— The processing of a pulse signal by a passive device is considered. A detailed analysis of the ultra-wideband (UWB) pulse propagation in two turns of meander microstrip line (MSL) connected in cascade is performed. The possibility of the UWB pulse decomposition in a meander MSL into a sequence of nine main pulses with 5.2 times attenuation is demonstrated. The conditions for such decomposition are determined and presented. A detailed description of each of the decomposition pulses at the end of the line under investigation is performed.

**Index Terms**—ultrashort pulse, meander line, protecting device, pulse train, even and odd mode

## I. INTRODUCTION

In modern science and technology, signal processing hardware based on numerical methods (digital signal processing) have become widespread in computer systems for analyzing, processing and generating pulse and harmonic signals. However, traditional hardware for analog signal processing based on active components, have relatively low speed, and often reliability, due to semiconductor components in their packaging [1]. Such components are highly susceptible to radiation, aging and have a limited operation cycle. Together with active signal processing devices, designers use passive devices, for example, the ones based on the printed circuit board strip transmission lines that are free from the most listed above disadvantages.

There are many studies of various devices based on strip lines for EMI protection and for signals filtering in the frequency domain [2–7]. There have been proposed a number of devices based on printed conductors, providing attenuation of ultra-wideband (UWB) pulses which are dangerous for sensitive REE. The possibility of attenuation is based on modal distortions of an UWB pulse by means of its decomposition into a sequence of pulses of smaller amplitude, which is less dangerous for sensitive REE circuits. Thus, an approach to attenuation is proposed, which is based on modal distortions of the signal in simple printed structures: meander delay lines [8, 9]. Basis of the approach is the UWB pulses decomposition into three main pulses in one turn of meander microstrip line (MSL). Decomposition is achieved by selecting line parameters that provide a number of simple conditions. Field tests of a device based on this approach were carried out, and the possibility of EE protecting against UWB pulses by the turn of meander MSL was experimentally proved [8]. The UWB pulse

decomposition at the end of meander line with broad-side coupling of two turns connected in cascade was also studied [9], but such investigation was not carried out for the meander MSL. Meanwhile, the possibility of decomposing an UWB pulse into a sequence of pulses after its propagating along the two turns may be used for signal processing, (for example, for generating a pulse train), and the meander lines can be used as passive devices for such processing. Then the aim of this paper is to investigate the possibility of UWB pulse decomposition in two turns of meander MSL connected in cascade.

## II. INITIAL DATA

The schematic diagram of two turns of meander MSL connected in cascade (Fig. 1) is the same as in [9].  $R1$  and  $R2$  are taken equal to the geometric means of the characteristic impedance of the first and second turn modes respectively. As an excitation, we used a pulse with following parameters from [9]:  $E=1$  V,  $t_f=100$  ps,  $t_r=t_f=50$  ps, where  $E$  – e.m.f. source,  $t_f$ ,  $t_r$ ,  $t_f$  – the flat top, rise and fall time durations. Turns of meander MSL have the same cross section, which is shown in Fig. 2.

It is known that the UWB pulse can be decomposed in a turn of a meander MSL into a sequence of cross-talk, odd and even modes pulses with a pulse-by-time separation of equal values [8]. The condition for such decomposition is

$$\tau_{max} \geq 2\tau_{min} \quad (1)$$

where  $\tau_{max}$  and  $\tau_{min}$  are the maximum and minimum values of per-unit-length delays of the line modes. Essentially, the condition (1) allows you to increase the duration of the UWB pulse decomposed in a meander MSL to a value equal to the product of the minimum of the per-unit-length delays and the line length.

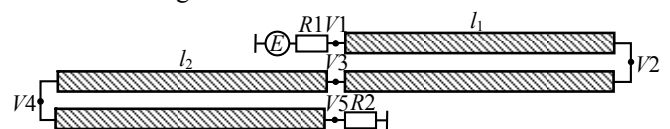


Fig. 1. Schematic diagram of a line under investigations

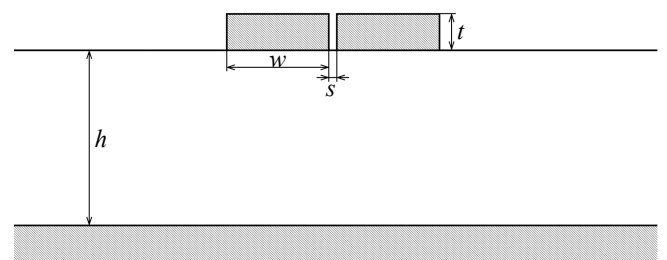


Fig. 2. Cross section of one turn of a meander MSL

Study was supported by the state contract 8.9562.2017/8.9 of the Ministry of Education and Science of the Russian Federation and the Russian Foundation for Basic Research grant 18-37-00339.

In order to complete UWB pulse decomposition in a line under investigation, first, it is necessary to decompose it in the first turn into crosstalk, odd and even modes pulses. Then it is necessary to decompose each of these pulses in the second turn into three similar pulses. Since a big number of reflections complicates the UWB pulse propagation in two turns, it is advisable to provide the condition (1) only in the first turn. This will exclude the superposition of the main decomposition pulses and reflected pulses and will minimize the UWB pulse amplitude.

To decompose the pulse sequence in the second turn, one must provide such delays of theirs in the second turn that will allow each of them to decompose into three pulses: crosstalk, odd and even modes. Also, it is necessary to consider their crosstalk from the output of the first turn (node  $V3$ ) to the output of the second turn (node  $V5$ ) whose delay at the end of the line is determined by the delay only in the first turn, since they are induced at the moment of pulse propagation in the second turn. At the end of meander MSL of two turns, there will also be a number of reflections from the junctions between the half-turns (nodes  $V2$  and  $V4$ ), turns (node  $V3$ ) and the line ends (nodes  $V1$  and  $V5$ ) which can overlap the main signal. Numerous simulation results obtained in the range of parameters have shown that to prevent partial overlapping it is necessary to provide the inequality in the second turn

$$\tau_{max} \geq 3\tau_{min}, \quad (2)$$

that will help to minimize the UWB pulse amplitude at the end of the line.

### III. PARAMETERS OF THE LINES

The simulation was performed using TALGAT system [10], which implements the calculation of transmission line parameter matrices with the method of moments and time response with the node-potential method [11]. Also, we note that the method of moments is widely used and proved itself to be good for simulation of meander delay lines [12–13].

According to condition (1), we performed the search for the optimal parameters of the first turn, which provide UWB pulse decomposition and minimization of its amplitude due to the optimal coupling between the first turn conductors. As a result of the search, we obtained the following cross-section parameters of the first turn: the width ( $w_1$ ) and thickness of the copper foil ( $t_1$ ) were 100  $\mu\text{m}$  and 160  $\mu\text{m}$ , respectively; the dielectric substrate thickness ( $h_1$ ) was 200  $\mu\text{m}$ ; the distance between conductors ( $s_1$ ) was 19.78  $\mu\text{m}$ ; the relative permittivity of the substrate ( $\epsilon_{r1}$ ) was 480. The calculated matrices  $\mathbf{C}$  and  $\mathbf{L}$  of the first turn were:

$$\mathbf{C} = \begin{bmatrix} 6.76 & -3.15 \\ -3.15 & 6.76 \end{bmatrix} \text{ nF/m}, \quad \mathbf{L} = \begin{bmatrix} 3.47 & 2.89 \\ 2.89 & 3.47 \end{bmatrix} \mu\text{H/m}.$$

The condition (2) in the second turn is ensured by the following parameters of the cross-section:  $w_2=400 \mu\text{m}$ ,  $t_2=600 \mu\text{m}$ ,  $h_2=200 \mu\text{m}$ ,  $s_2=20.2592 \mu\text{m}$ ,  $\epsilon_{r2}=120$ . The calculated matrices  $\mathbf{C}$  and  $\mathbf{L}$  of the second turn were:

$$\mathbf{C} = \begin{bmatrix} 3.58 & -1.06 \\ -1.06 & 3.58 \end{bmatrix} \text{ nF/m}, \quad \mathbf{L} = \begin{bmatrix} 1.63 & 1.45 \\ 1.45 & 1.63 \end{bmatrix} \mu\text{H/m}.$$

By means of the  $\mathbf{C}$  and  $\mathbf{L}$  matrices, we obtained the per-unit-length delays of first and second turns modes [14]:

$\tau_{e1}=47.88 \text{ ns/m}$ ,  $\tau_{e2}=27.88 \text{ ns/m}$ ,  $\tau_{o1}=23.94 \text{ ns/m}$ ,  $\tau_{o2}=9.29 \text{ ns/m}$ . After pre-simulation of the time response, we determined preliminary values of the turn lengths to prevent the overlapping of the decomposition pulses: the length ( $l_1$ ) of the first turn is 45 mm, and of the second one ( $l_2$ ) is 25 mm.

### IV. TIME RESPONSE

Fig. 3 shows the signal waveform at the end of the first turn ( $V3$ ) when condition (1) was fulfilled.

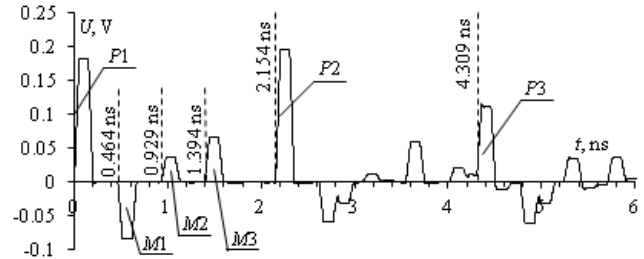


Fig. 3. Waveform at node  $V3$  when condition (1) was fulfilled

From Fig. 3 we can see that the signal at the first turn end is presented as a sequence: cross-talk ( $P1$ ), odd ( $P2$ ) and even ( $P3$ ) modes. It is also seen that the delay of the even mode pulse is twice ( $\tau_{e1}l_1=47.87 \text{ ns/m} \cdot 45 \text{ mm}=2.154 \text{ ns}$ ) as big as the delay of the odd mode pulse (these values are noted in the diagram). The amplitude of the signal at node  $V3$  is 196 mV. The diagram in Fig. 3 also contains pulses (between  $P1$  and  $P2$ , and between  $P2$  and  $P3$  pulses) caused by the reflections. As an example, we consider details of the  $M1$ ,  $M2$  and  $M3$  pulses caused by the reflections. In fact,  $M1$  (odd mode) and  $M3$  (even mode) are the results of the decomposition in the second turn of the crosstalk pulse reflected from the end of the line, which came to the end of the second turn (node  $V5$ ) from node  $V1$ , while the pulse  $M2$ , as a result of reflection from the junction between turns, is actually the  $M1$  pulse which twice passed through the second turn. Therefore, the delays of  $M1$ ,  $M2$ ,  $M3$  pulses can be defined as  $t_{M1}=\tau_{o2} \cdot 2l_2=0.464 \text{ ns}$ ,  $t_{M2}=\tau_{o2} \cdot 4l_2=0.929 \text{ ns}$ ,  $t_{M3}=\tau_{e2} \cdot 2l_2=1.394 \text{ ns}$ . Fig. 4 shows the voltage waveform of the signal at the end of the meander MSL of two turns when conditions (1) and (2) are fulfilled in the first and second turns respectively.

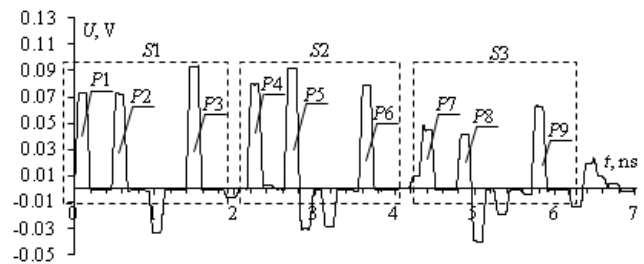


Fig. 4. Waveform at node  $V5$  when conditions (1) and (2) are fulfilled in the first and second turns respectively

From Fig. 4 we can see that the UWB pulse at the end of line under investigation is presented by three sequences of pulses ( $S1$ ,  $S2$ ,  $S3$ ) of smaller amplitude, not exceeding the 94 mV. Sequence  $S1$  is the result of the crosstalk pulse (induced from node  $V1$  to node  $V3$ ) decomposition into odd ( $P2$ ) and even ( $P3$ ) mode pulses in the second turn.

Sequence  $S2$  is the decomposition of odd mode pulse from the first turn ( $P2$  in Fig. 3) into the odd ( $P2$ ) and even ( $P3$ ) mode pulses in the second turn, and  $S3$  is the decomposition of even mode pulse from the first turn ( $P3$  in Fig. 3) into the odd ( $P2$ ) and even ( $P3$ ) mode pulses in the second turn. Pulses  $P1$ ,  $P4$  и  $P7$  are crosstalk pulses at node  $V5$  from crosstalk pulse (first induced from node  $V1$  to node  $V3$  and then to node  $V5$ ), as well as from odd and even modes pulses of the first turn ( $P2$  and  $P3$  in Fig. 3) respectively. Also, from Fig. 4 one can see many pulses of smaller amplitude (compared to the main pulses of the three sequences) caused by reflections. As a result, the amplitude attenuation of the UWB pulse at the end of the line of is 5.2 times.

To completely understand the process of pulse decomposition in two turns of meander MSL connected in cascade, Table I summarizes the delays of each of the main pulses ( $P1$ – $P9$ ) of three sequences ( $S1$ – $S3$ ) at the end of the line (Fig. 4), where  $t_c$  (we use indexes  $c$  for crosstalk,  $e$  for even and  $o$  for odd modes) is the first pulse delay,  $t_{co}$  is the second pulse delay,  $t_{ce}$  is the third pulse delay,  $t_{oc}$  is the fourth pulse delay,  $t_{oo}$  is the fifth pulse delay,  $t_{oe}$  is the sixth pulse delay,  $t_{ec}$  is the seventh pulse delay,  $t_{eo}$  is the eighth pulse delay,  $t_{ee}$  is the ninth pulse delay (where indexes  $co$  is an odd mode from crosstalk in node  $V3$ ,  $ce$  is an even mode from crosstalk in node  $V3$ ,  $oc$  is crosstalk in node  $V5$  from an odd mode pulse from the first turn,  $oo$  is an odd mode from odd mode pulse of the first turn,  $oe$  is an even mode from an odd mode pulse of the first turn,  $ec$  is a crosstalk pulse in node  $V5$  from an even mode from the first turn,  $eo$  is an odd mode from an even mode pulse of the first turn,  $ee$  is an even mode from an even mode pulse of the first turn). Whereas the first sequence is a result of the crosstalk pulse decomposition into the crosstalk pulse and the odd and even mode pulses only in the second turn, the delay of the first pulse is defined as  $t_c=0$  ns, second pulse delay is  $t_{co}=\tau_{o2}\cdot 2l_2$  (where  $\tau_{o2}$  is per-unit-length delay of odd mode of the second turn, a  $l_2$  is length of the second turn), and the third is  $t_{ce}=\tau_{e2}\cdot 2l_2$  (where  $\tau_{e2}$  is per-unit-length delay of the even mode of the second turn). The second pulse sequence is a result of the decomposition of the odd mode pulse from the first turn ( $P2$  in Fig. 3) into the crosstalk pulse and the odd and even mode pulses in the second turn, so the delay of the fourth pulse is defined as  $t_{oc}=\tau_{o1}\cdot 2l_1$  (where  $\tau_{o1}$  is per-unit-length delay of the odd mode of the first turn,  $l_1$  is length of the first turn), and the fifth pulse delay is  $t_{oo}=\tau_{o1}2l_1+\tau_{o2}2l_2$ , and the sixth is  $t_{oe}=\tau_{o1}2l_1+\tau_{e2}2l_2$ . The third sequence of pulses is the result of the decomposition of the even mode pulse from the first turn ( $P3$  in Fig. 3) in the second turn, then the delay of the seventh pulse is defined as  $t_{ec}=\tau_{e1}2l_1$  (where  $\tau_{e1}$  is per-unit-length delay of even mode of the first turn), and the eighth pulse delay is  $t_{eo}=\tau_{e1}2l_1+\tau_{o2}2l_2$ , and the ninth is  $t_{ee}=\tau_{e1}2l_1+\tau_{e2}2l_2$ .

TABLE I. DELAYS (NS) OF EACH OF THE MAIN PULSES OF 3 SEQUENCES AT THE END OF THE LINE UNDER INVESTIGATION

$S1 (P1-P3)$			$S2 (P4-P6)$			$S3 (P7-P9)$		
$t_c$	$t_{co}$	$t_{ce}$	$t_{oc}$	$t_{oo}$	$t_{oe}$	$t_{ec}$	$t_{eo}$	$t_{ee}$
0	0.46	1.39	2.15	2.61	3.54	4.3	4.77	5.69

Based on the above considerations, it follows that in order to completely decompose the signal, that came from the first turn into the second turn, it is necessary for the delay of each of the main pulses of the three sequences (with the exception of  $P1$ ) in the line to be more than the delay of the previous pulse summed with the duration of the UWB pulse, otherwise the pulses will overlap each other. This can be provided by the following set of conditions:

$$t_{co} \geq t_{\Sigma}, \quad (3)$$

$$t_{ce} \geq t_{co} + t_{\Sigma}, \quad (4)$$

$$t_{oo} \geq t_{oc} + t_{\Sigma}, \quad (5)$$

$$t_{oe} \geq t_{oo} + t_{\Sigma}, \quad (6)$$

$$t_{eo} \geq t_{ec} + t_{\Sigma}, \quad (7)$$

$$t_{ee} \geq t_{eo} + t_{\Sigma}, \quad (8)$$

where  $t_{\Sigma}$  is the sum of rise, fall and top times of the source.

If we know how to determine the delays of each of the main pulses of the sequences ( $t_c, t_{co}, \dots, t_{ee}$ ), then after simple algebraic transformations, the conditions (3), (5) and (7) will take the following similar form

$$2l_2\tau_{o2} \geq t_{\Sigma}, \quad (9)$$

and conditions (4), (6) and (8) will have the following similar form

$$2l_2|\tau_{e2} - \tau_{o2}| \geq t_{\Sigma}. \quad (10)$$

Then, to prevent the main signal from overlapping the crosstalk pulse in each pulse sequence ( $S1$ – $S3$ ) in Fig. 4, it is enough to provide condition (9), and for the decomposition of the main signal into pulses of odd and even modes – condition (10). After substituting the values in condition (9) we obtain  $0.46 \text{ ns} \geq 0.2 \text{ ns}$ , and in condition (10) –  $0.93 \text{ ns} \geq 0.2 \text{ ns}$ . Thus, conditions (9) and (10) are fulfilled with a margin.

It is important to note, that  $P3$  can overlap  $P4$ , and  $P6$  can overlap  $P7$ , for example, when the UWB pulse has a longer duration or when the second turn has a longer length. To avoid this, it is necessary to additionally provide the conditions

$$t_{oc} \geq t_{ce} + t_{\Sigma}, \quad (11)$$

$$t_{ec} \geq t_{oe} + t_{\Sigma}. \quad (12)$$

After simple algebraic transformations, the condition (11) takes the following form

$$2l_1\tau_{o1} - 2l_2\tau_{e2} \geq t_{\Sigma}, \quad (13)$$

and condition (12) takes the following form

$$2l_1(\tau_{e1} - \tau_{o1}) - 2l_2\tau_{e2} \geq t_{\Sigma}. \quad (14)$$

After substituting the values in conditions (13) we obtain  $0.76 \text{ ns} \geq 0.2 \text{ ns}$ , and in condition (14) –  $0.76 \text{ ns} \geq 0.2 \text{ ns}$ .

Thus, conditions (13) and (14) are performed with a margin. But, it is important to note that the calculated values of the left-hand sides of (13) and (14) are the same. It is due to the fact that the condition (1) in the first turn is fulfilled, with the maximum of even and odd mode per-unit-length delays of the first turn being equal to a doubled minimum of the even and odd mode per-unit-length delays of the first turn.

To confirm the conditions (9), (10), (13) and (14), it is worth considering the case when the conditions are not fulfilled. Let us consider the case, when the condition (9) is not performed, for example, by decreasing  $l_2$ . Fig. 5 shows the waveforms at the end of the considered line with the length of the second turn of 10 and 5 mm, and 45 mm for the first turn.

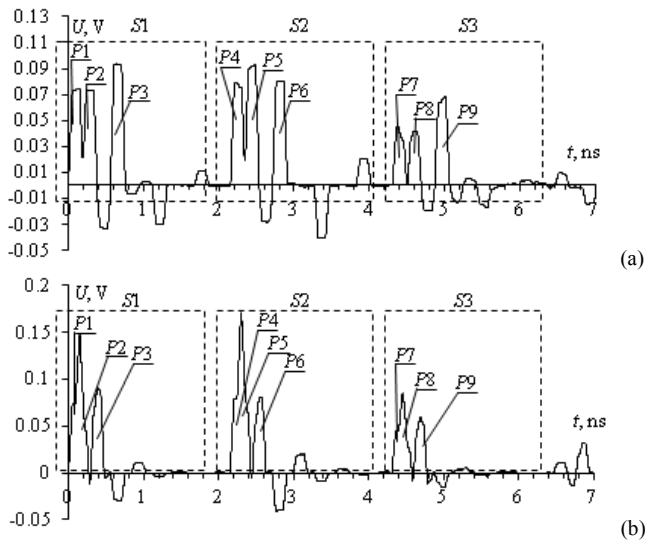


Fig. 5. Waveforms at node  $V_5$  for  $l_2=10$  (a), 5 (b) mm

From the waveforms in Fig. 5 it can be seen that when the length of the second turn decreases to 10 mm, the rises of the odd mode pulses ( $P_2, P_5, P_8$  in Fig. 5a) begin to overlap the crosstalk pulses ( $P_1, P_4, P_7$  in Fig. 5a). In this case, the signal amplitude at node  $V_5$  for  $l_2=10$  mm does not exceed 94 mV either, since it is still determined by the  $P_3$  pulse amplitude. However, for  $l_2=5$  mm (Fig. 5b), the signal amplitude at node  $V_5$  already is 171 mV. So, for  $l_2=10$  mm the condition (9) is not fulfilled ( $0.18 \text{ ns} \leq 0.2 \text{ ns}$ ), the same is also true for  $l_2=5$  mm ( $0.093 \text{ ns} \leq 0.2 \text{ ns}$ ).

Next we consider the case, when the condition (10) is not fulfilled, for example, by decreasing  $\epsilon_{r2}$  value to 5 (for  $l_2=25$  mm), then  $0.12 \text{ ns} \leq 0.2 \text{ ns}$ . Fig. 6 shows the waveforms at the end of the considered line for  $\epsilon_{r2}=5$ .

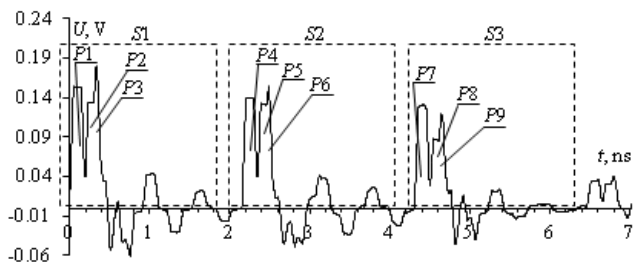


Fig. 6. Waveforms at node  $V_5$  for  $\epsilon_{r2}=5$

It can be seen from the waveforms in Fig. 6 that the main pulses of the three sequences are not decomposed into pulses of odd ( $P_2, P_5, P_8$ ) and even ( $P_3, P_6, P_9$ ) modes. Herewith, the amplitude of the signal at node  $V_5$  is 180 mV.

Finally, consider the case when conditions (13) and (14) are not fulfilled, for example, by increasing  $l_2$  to 35 mm and increasing the UWB pulse duration to 0.3 ns. Signal waveforms at the end of two turns of meander MSL connected in cascade for  $l_2=35$  mm and UWB pulse duration of 0.3 ns are shown in Fig 7.

From the waveforms in Fig. 7 it can be seen that the even mode pulse of the first sequence ( $P_3$ ) overlaps the crosstalk pulse of the second sequence ( $P_4$ ), and the even mode pulse of the second sequence ( $P_6$ ) overlaps the crosstalk pulse of the third sequence ( $P_7$ ). The signal amplitude at node  $V_5$  is 168 mV. As a result of substituting the values of the variables in (13) and (14), we obtain for either condition  $0.2 \text{ ns} \leq 0.3 \text{ ns}$ .

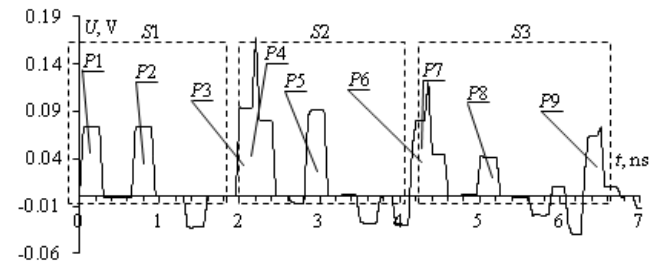


Fig. 7. Waveforms at node  $V_5$  for  $l_2=35$  mm and the UWB pulse duration of 0.3 ns

Concerning the validation of the obtained results, we note the following. This paper is the first step in the study of two turns of meander MSL connected in cascade as analog devices for the division of one UWB pulse into a sequence (pulse train). Therefore, the paper was not anticipated the comparison of the obtained results with the results obtained by the other numerical methods, by other software products and experimentally. Meanwhile, the available groundwork in the study of a meander MSL turn confirms the correctness of the numerical method and software used for the simulation of similar devices. Thus, a good agreement of the time and frequency characteristics of a meander line turn obtained from simulation and experiment has been shown [8]. In addition, the consistent results of quasistatic and electrodynamic simulation of meander MSL has been presented [15].

## V. CONCLUSIONS

In this paper, we demonstrated the feasibility of UWB pulse decomposition into a sequence of pulses of smaller amplitude in two turns of meander MSL connected in cascade. Since the condition (1) in the first turn and (2) in the second turn were fulfilled, we obtained the UWB pulse amplitude attenuation of 5.2 times at the line end. We also formulated a number of conditions that provide the decomposition of each of the pulse sequence from the end of the first turn in the second turn, and make it possible to prevent the even mode pulses of each sequence from overlapping the following sequence crosstalk pulse. It is worth mentioning, that the optimal parameters that provide required conditions are difficult to implement in practice. However, it is possible to fulfill the corresponding conditions in the first and second turns by choosing values of other cross-section parameters. For example, this can be executed through optimization with genetic algorithms that provides the possibility to set the required range of parameters to be optimized. Nevertheless, the presented results allow us to confirm that when the corresponding conditions are fulfilled in the first and second turns, it is possible to minimize the UWB pulse amplitude in two turns of the meander MSL connected in cascade by its

decomposition into a crosstalk pulse and the odd and even mode pulses first in the first turn, and then, similarly, each of them in the second turn.

The considered phenomenon and the corresponding structures can be used for noise protection in the form of filtering devices based on meander lines. For example, this phenomenon may be useful for sensitive REE testing, when the testing is required for the effects of a series (pulse train) of UWB pulses that sequentially arrive at the input of devices. The implementation of such dividing devices is seen as an intermediate part connected to the output of the generator, before entering the test object.

#### REFERENCES

- [1] Z.M. Gizatullin, R.M. Gizatullin, "Investigation of the immunity of computer equipment to the power-line electromagnetic interference," *Journal of Communications Technology and Electronics*, no. 5, pp. P. 546–550, 2016.
- [2] R. Krzikalla, J.L. ter Haseborg, F. Sabath, "Systematic description of the protection capability of protection elements," *Proc. of IEEE Int. Symp. on EMC, Honolulu, HI, USA*, pp. 1–4, 2007.
- [3] R. Krzikalla, T. Weber, J.L. ter Haseborg, "Interdigital microstrip filters as protection devices against ultrawideband pulses," *Proc. of IEEE Int. Symp. on EMC, Istanbul, Turkey*, pp. 1313–1316, 2003.
- [4] R. Krzikalla, J.L. ter Haseborg, "SPICE simulations of uwb pulse stressed protection elements against transient interferences," *Proc. of IEEE Int. Symp. on EMC, Chicago, IL, USA*, pp. 977–981, 2005.
- [5] T. Weber, R. Krzikalla, J.L. Haseborg, "Linear and nonlinear filters suppressing UWB pulses," *IEEE Trans. on EMC*, vol. 36, no. 3, pp. 423–430, 2004.
- [6] Q. Cui, S. Dong, Y. Han, "Investigation of waffle structure SCR for electrostatic discharge (ESD) protection" *IEEE International Conference on Electron Devices and Solid State Circuit (EDSSC)*, 2012, Bangkok, Thailand, p. 4, 3–5 Dec. 2012.
- [7] H. Hayashi, T. Kuroda, K. Kato, K. Fukuda, S. Baba, Y. Fukuda, "ESD protection design optimization using a mixed-mode simulation and its impact on ESD protection design of power bus line resistance," *International Conference on Simulation of Semiconductor Processes and Devices, 2005 (SISPAD 2005)*, Tokyo, Japan, pp. 99–102, Sept. 2005.
- [8] R.S. Surovtsev, A.V. Nosov, A.M. Zabolotsky, T.R. Gazizov, "Possibility of protection against UWB pulses based on a turn of a meander microstrip line," *IEEE Transactions on Electromagnetic Compatibility*, vol. 59, no. 6, pp. 1864–1871, Dec. 2017.
- [9] A.V. Nosov, R.S. Surovtsev, "Ultrashort Pulse Decomposition in Meander Line with Broad-Side Coupling of Two Turns," *20th International Conference of Young Specialists on Micro/Nanotechnologies and Electron Devices*, pp. 83–87, June 29 – July 3 2019.
- [10] S.P. Kuksenko, "Preliminary results of TUSUR University project for design of spacecraft power distribution network: EMC simulation," *IOP Conference Series: Materials Science and Engineering*, vol. 560, no. 1, pp. 1–6, 2019.
- [11] J.R. Griffith, M.S. Nakhla, "Time-domain analysis of lossy coupled transmission lines," *IEEE Transactions on Microwave Theory and Techniques*, vol. 38, no. 10, pp. 1480–1487, 1990.
- [12] B.J. Rubin, B. Singh, "Study of meander line delay in circuit boards," *IEEE Trans. on Microwave Theory and Techniques*, vol. 48, pp. 1452–1460, 2000.
- [13] A.U. Bhobe, C. Lolloway, M. Picket-May, "Meander delay line challenge problems: a comparison using FDTD, FEM and MoM," *Int. Symposium on EMC*, pp. 805–810, 2001.
- [14] N.D. Malyutin, "Mnogosvyaznyye poloskovyye struktury i ustroystva na ikh osnove," *Tomsk: Izd-vo Tom. un-ta*. 1990, 164 s. (in Russian).
- [15] P.E. Orlov, T.R. Gazizov, A.M. Zabolotsky, "Short pulse propagation along microstrip meander delay lines with design constraints: comparative analysis of the quasi-static and electromagnetic approaches," *Applied computational electromagnetics society journal*, vol. 31, no. 3. pp. 238–243, 2016.